NASA TM-87584

NASA Technical Memorandum 87584

NASA-TM-87584 19850026113

NONLINEAR ADHESIVE BEHAVIOR EFFECTS IN A CRACKED ORTHOTROPIC SHEET STIFFENED BY A SEMI-INFINITE ORTHOTROPIC SHEET

C. A. BIGELOW

AUGUST 1985

National Aeronautics and Space Administration

Langley Research Center
Hampton, Virginia 23665

SUMMARY

Although stringers are used primarily as stiffeners, they also can make damaged structures fail-safe or damage tolerant. Assessment of the damage tolerance of structures weakened by cracks is aided by knowledge of stress-intensity factors. In this paper, the stress-intensity factor is determined for a cracked orthotropic sheet adhesively bonded to an orthotropic stringer where the adhesive layer is modeled with a nonlinear stress-strain curve. Since the stringer is modeled as a semi-infinite sheet, the solution is most appropriate for a crack tip located near a stringer edge. Both adherends are treated as homogeneous, orthotropic media which are representative of many fiber-reinforced composite materials. It was assumed that the adherends are in a state of plane stress and the adhesive is in pure shear. By the use of Green's functions and the complex variable theory of orthotropic elasticity developed by Lekhnitskii, a set of integral equations is obtained. The integral equations are replaced by an equivalent set of algebraic equations, which is solved to obtain the shear stress distribution in the adhesive layer. With these adhesive stresses, the crack-tip stress-intensity factors are found.

The effect of adhesive nonlinearity on the adhesive shear stress distribution and the stress-intensity factors is examined. When the adhesive was modeled with a nonlinear stress-strain curve, the peak shear stresses in the adhesive were considerably reduced in comparison to the solution for the linear elastic adhesive. This resulted in increases in the stress-intensity factors for the nonlinear adhesive solution compared to the linear adhesive solution. When the adhesive behaved nonlinearly, less load was transferred from the infinite sheet to the stringer, and thus the stringer was less effective in reducing the crack-tip stress-intensity factors. The adhesive nonlinearity had

less effect on the stress-intensity factors at the crack tip farthest from the stringer than on the stress-intensity factors at the crack tip nearest the stringer, and the nonlinear adhesive did not have a signifi-cant effect on the stress-intensity factor unless the near crack tip was beneath the stringer. The present investigation assumes that the adhesive bond remains intact. Onset of adhesive failure is predicted to occur at decreasing levels of applied stress as the crack propagates beneath the stringer.

INTRODUCTION

Structural configurations proposed for composite airplanes have typically been very similar to the sheet-stringer construction widely used in metal airplanes. In metal airplanes, stringers have been shown to be effective in making damaged structures fail-safe or damage tolerant. A stringer retards crack growth by increasing the stiffness of the structure. As a crack tip approaches a stringer, debonding of the adhesive may start or the crack may extend beneath the stringer without debonding, depending on the relative crack-growth resistance of the structure and the adhesive. Additionally, the adhesive may exhibit large regions of nonlinear behavior. These phenomena affect the state of stress at the crack tip and, thus, the effectiveness of the stringer in reducing the rate of crack propagation in the structure. The interaction of a through-the-thickness crack and a stringer is an important problem and has been investigated by many authors.

A brief summary of some of the recent work dealing with the sheet-stringer construction begins with the work of Arin (ref. 1), where he examined the effect of a partially debonded, infinite stringer on the stress-intensity factor for the crack. He found that the stringer exerts little influence on the stress-intensity factor unless it is quite close to the crack tip. How-ever, since he

assumed that the stringer was adhesively bonded to the sheet along a line perpendicular to the crack, his solution was unable to model cracks growing beneath the stringer. Swift (ref. 2) presented a closed form solution for the analysis of riveted stringer panels including the effects of fastener flexibility and stiffener bending. He found that considereable error in the crack-tip stress intensities and the stiffener stress concentrations could result if fastener flexibility was not accounted for. Anderson, Chu and McGee (ref. 3) considered the growth characteristics of a fatigue crack approaching and growing beneath an adhesively bonded stringer. In this work, a two-dimensional finite element analysis was used to compute the stress-intensity factor as a function of crack length for linear and nonlinear repre-sentations of the adhesive. The nonlinear representation of the adhesive predicted debond areas that agreed extremely well with the experimentally observed debond. The nonlinearity of the adhesive, combined with debonding, also reduced the stress-intensity factor relative to the linear elastic solution. Their work dealt only with isotropic adherends.

Hart-Smith (ref. 4) developed analysis methods for determining adhesive bond stresses in stringer panels. His analysis pointed to the need to account for adhesive plasticity and stiffener yielding. He considered only metal elements in three configurations. Swift (ref. 5) used a simple, pseudo-closed form approach to account for plasticity in the stringer and adhesive layer. He considered only isotropic materials in a single configuration and found that modeling the elastic-plastic behavior of both the adhesive and the stiffener was essential in predicting the failure mode.

Thus, there is ample evidence to indicate the need for modeling the non-linearity of the adhesive in bonded structures. However, no previous analytic

work has considered the problem of orthotropic materials bonded with a nonlinear adhesive. Here the problem of a semi-infinite orthotropic sheet adhesively bonded to an infinite, cracked orthotropic sheet with a nonlinear adhesive is considered. The semi-infinite sheet is referred to as a stringer for convenience.

In reference 6, the solution to this problem assuming a linear elastic adhesive was presented. The parameter having the greatest influence on the stress-intensity factors was found to be the distance from the near crack tip to the edge of the stringer. Unless the crack tip was very close to or under the stringer, the stress-intensity factor was approximately that of an un-stifffened sheet. However, as the crack propagated beneath the stringer, the stress-intensity factor decreased significantly. Increasing the stringer stiffness or increasing the adhesive stiffness also resulted in a decrease in the stress-intensity factor.

In the present work, a nonlinear stress-strain curve for the adhesive is used the analysis. First, the formulation of the integral equations des-cribing the problem is briefly reviewed. These integral equations are replaced by an equivalent set of algebraic equations, which is solved to obtain the shear stress distribution in the adhesive layer. Because of the nonlinear stress-strain behavior of the adhesive, these equations are solved in an iterative fashion. Once these adhesive stresses are known, the stress-intensity factors at both crack tips are found. The effects of the nonlinear stress-strain curve of the adhesive on the adhesive stresses and on the stress-intensity factors are presented and discussed.

NOMENCLATURE

a	half-crack length, m
b	distance from edge of stringer to center of crack, m
D	domain of integration
f_{01}, f_{02}	stress functions, m^3/N
G_3	tangent shear modulus of adhesive layer, Pa
h_j	thickness of layer j, m
k_1	mode I component of stress-intensity factor, $Pa\sqrt{m}$
N	number of cells or collocation points in the domain
S_{jk}	complex kernels in integral equations (j,k=1,2), 1/(Pa*m)
x, y	Cartesian coordinates
x_0, y_0	coordinates of concentrated load point, m
z_j	complex variable (j=1,2), m
Δx_j, Δy_j	incremental distances (j=1,N), m
γ_x, γ_y	shear strains
σ_0	crack-face pressure, Pa
τ	shear stress, Pa
τ_x, τ_y	adhesive shear stresses, Pa

Superscripts:

(j)	layer number (j=1,2)

FORMULATION OF THE PROBLEM

Consider the stringer configuration shown in figure 1. The semi-infinite sheet is referred to as a stringer for convenience. The stringer and the

infinite sheet are bonded together with a adhesive layer of constant thickness h_3. The adhesive is assumed to remain intact throughout the analysis. The stress-strain curve of the adhesive is assumed to be nonlinear elastic. Both the infinite sheet and the stringer are made of a fiber-reinforced composite which is treated as a homogenous, orthotropic, linearly elastic medium. The infinite sheet consists of a quasi-isotropic laminate and the stringer has a unidirectional layup. The material properties are given in table I (ref. 7).

The model is loaded by a uniform pressure σ_0 on the crack faces so that the stress state at infinity is zero. If the two layers have equal inplane Poisson's ratios, ν_{yx}, the stress-intensity factor solution presented here for the uniformly stressed crack face is identical to the problem of the remotely loaded stringer panel. On the other hand, if $\nu_{yx}^{(1)} \neq \nu_{yx}^{(2)}$, as is the case here, the displacements in the x-direction will differ for the two loading cases, and therefore the two solutions will not be equivalent. However, it was shown in ref. 8 that the differences in the two solutions are not large. For the materials considered here, the error introduced by this approximation is less than 5%. Thus, the present solution for a uniformly stressed crack face is a close approximation to the solution for the corresponding case with remote loading.

By use of Green's functions and the complex variable theory of orthotropic elasticity developed by Lekhnitskii, a set of integral equations describing the problem was formulated (ref. 6). For elastic linear adhesive behavior, the problem in figure 1 was reduced to the solution of these integral equa-tions, shown below in equations (1). The development of these equations is briefly reviewed in appendix A.

$$\frac{h_3}{G_3}\ \tau_x(x,y) + \iint_D [S_{11}(x,y,x_0,y_0)\ \tau_x(x_0,y_0) + S_{12}(x,y,x_0,y_0)\ \tau_y(x_0,y_0)]\ dx_0\ dy_0 = \sigma_0\ f_{01}(x,y)$$

$$\frac{h_3}{G_3}\ \tau_y(x,y) + \iint_D [S_{21}(x,y,x_0,y_0)\ \tau_x(x_0,y_0) + S_{22}(x,y,x_0,y_0)\ \tau_y(x_0,y_0)]\ dx_0\ dy_0 = \sigma_0\ f_{02}(x,y) \qquad (1)$$

Here τ_x and τ_y are the unknown adhesive shear stresses in the x- and y-directions, respectively, and the kernels S_{jk} (j,k=1,2) and the functions f_{01} and f_{02} are known (see appendix A); D is the region of the adhesive bond and G_3 is the tangent shear modulus of the adhesive.

The nonlinearity of equations (1) is accounted for by G_3, the tangent shear modulus; the value of G_3 depends on the current state of stress in the adhesive. Following the procedure used in reference 9, the quantities τ_x/G_3 and τ_y/G_3 are replaced by the shear strains, γ_x and γ_y. Thus, the integrals of equations (1) are now rewritten as follows:

$$h_3\ \gamma_x(x,y) + \iint_D [S_{11}(x,y,x_0,y_0)\ \tau_x(x_0,y_0) + S_{12}(x,y,x_0,y_0)\ \tau_y(x_0,y_0)]\ dx_0\ dy_0 = \sigma_0\ f_{01}(x,y)$$

$$h_3\ \gamma_y(x,y) + \iint_D [S_{21}(x,y,x_0,y_0)\ \tau_x(x_0,y_0) + S_{22}(x,y,x_0,y_0)\ \tau_y(x_0,y_0)]\ dx_0\ dy_0 = \sigma_0\ f_{02}(x,y) \qquad (2)$$

The solution of equations (2) will produce the shear stress distribution in the adhesive, τ_x and τ_y. With these adhesive stresses, the stress-intensity factor at either crack tip can be found. The solution of these equations will be discussed in the next section.

NUMERICAL SOLUTION OF THE INTEGRAL EQUATIONS

A key item in the analysis is the method of integration used for the system of integral equations represented by equations (2). Since the kernels S_{jk} (j,k=1,2) contain only logarithmic singularities and are integrable in the infinite domain D, equations (2) can be treated as Fredholm equations of the second kind. Due to the complicated nature of these equations, a closed form integration is difficult if not impossible to perform. Consequently, the system of equations is solved using standard numerical techniques. This is done by dividing the domain D into cells assuming the unknown functions τ_x and τ_y to be uniform in each cell and then using a numerical scheme to evaluate the equations.

The outer boundary of the domain D theoretically goes to infinity. However, in order to carry out the numerical analysis, the size of D must be restricted. A convergence study was conducted to determine the extent and refinement necessary so that the critical quantities of interest, the stress-intensity factors, were not appreciably affected by the restriction. Thus, for the linear elastic adhesive solution (ref. 6), the size of D was deter-mined iteratively, starting with a small, coarse mesh and increasing the extent and refinement until no significant changes occurred in the stress-intensity factor. A typical mesh layout used in reference 6 is shown in figure 2, where, because of symmetery, only one half of the integration domain is shown. The same meshes

are used in the current analysis for the nonlinear representation of the adhesive.

When the integrals in equations (2) are replaced by summations, the following system of linear algebraic equations is obtained:

$$h_3\,\gamma_x(x_j,y_j) + \sum_{n=1}^{N} [S_{11}(x_j,y_j,x_{0_n},y_{0_n})\,\tau_x(x_{0_n},y_{0_n}) + S_{12}(x_j,y_j,x_{0_n},y_{0_n})\,\tau_y(x_{0_n},y_{0_n})]\,\Delta x_n\,\Delta y_n = \sigma_0\,f_{01}(x_j,y_j) \tag{3}$$

$$h_3\,\gamma_y(x_j,y_j) + \sum_{n=1}^{N} [S_{21}(x_j,y_j,x_{0_n},y_{0_n})\,\tau_x(x_{0_n},y_{0_n}) + S_{22}(x_j,y_j,x_{0_n},y_{0_n})\,\tau_y(x_{0_n},y_{0_n})]\,\Delta x_n\,\Delta y_n = \sigma_0\,f_{02}(x_j,y_j) \qquad (j = 1,N)$$

where

N = number of collocation points or the number of cells in the domain.

For the linear elastic representation of the adhesive, these equations would only need to be solved a single time. However, when a nonlinear stress-strain curve is used to model the adhesive, these equations are solved iteratively using a linear piece-wise approximation of the adhesive stress-strain curve. Assuming that the adhesive stress-strain curve is given in tabular form, the relationship between the stress and the strain can be obtained by linear interpolation (ref. 9). Let τ be the unknown stress on the stress-strain curve (figure 3), and τ_{j-1} and τ_j are the adjacent points given on the stress-strain curve such that $\tau_{j-1} \leq \tau \leq \tau_j$, and the corresponding shear strains are $\gamma_{j-1} \leq \gamma \leq \gamma_j$. As shown in figure 3, the relationship between γ and τ can be written as follows:

$$\gamma = \gamma_{j-1} + (\tau - \tau_{j-1}) \frac{\gamma_j - \gamma_{j-1}}{\tau_j - \tau_{j-1}} \tag{4}$$

This equation will be rewritten as

$$\gamma = m\tau + d \tag{5}$$

where

$$m = \frac{\gamma_j - \gamma_{j-1}}{\tau_j - \tau_{j-1}}$$

$$d = \gamma_{j-1} - m\tau_{j-1} \tag{6}$$

To obtain a system of equations where the only unknowns are the shear stresses, τ_x and τ_y, equation (5) is substituted into equations (3) which are now rewritten as the following:

$$h_3 m_x \tau_x(x_j,y_j) + \sum_{n=1}^{N} [S_{11}(x_j,y_j,x_{0_n},y_{0_n}) \tau_x(x_{0_n},y_{0_n}) + S_{12}(x_j,y_j,x_{0_n},y_{0_n}) \tau_y(x_{0_n},y_{0_n})] \Delta x_n \Delta y_n = \sigma_0 f_{01}(x_j,y_j) - h_3 d_x \tag{7}$$

$$h_3 m_y \tau_y(x_j,y_j) + \sum_{n=1}^{N} [S_{21}(x_j,y_j,x_{0_n},y_{0_n}) \tau_x(x_{0_n},y_{0_n}) + S_{22}(x_j,y_j,x_{0_n},y_{0_n}) \tau_y(x_{0_n},y_{0_n})] \Delta x_n \Delta y_n = \sigma_0 f_{02}(x_j,y_j) - h_3 d_y$$

$$(j = 1,N)$$

where m_x, m_y and d_x, d_y correspond to the adhesive shear stresses τ_x and τ_y.

Equations (7) can now be solved successively for the shear stresses τ_x and τ_y. The iteration continues until the correct slope of the stress-strain curve, for the given level of applied stress, is found. The maximum shear stress criterion is used to determine the correct slope for a given level of applied stress. In this criterion, it is assumed that there is no interaction between the x- and y-components of the shear stress. The solution was found to converge very quickly, typically within 5 to 10 iterations, depending upon the level of the applied stress. Equations (7) show that the kernels S_{jk} are constant throughout the iteration process and need to be calculated only once. The terms, m_x, m_y, and d_x, d_y, depend on the current stress level and must be calculated again within each iteration.

NUMERICAL RESULTS

The system of equations given by (7) is solved to produce the adhesive stresses. These stresses are then used to calculate the stress-intensity factors, k_1, using equation (A.4) given in appendix A. In the examples considered here, the infinite sheet is modeled as a graphite/epoxy laminate with a quasi-isotropic layup and the stringer is modeled as a unidirectional graphite/epoxy laminate. The material properties are shown in table I (ref. 7). The thickness of the infinite sheet h_1 is chosen as 2.0 mm and the thick-ness of the stringer h_2 is 1.0 mm. The stress-strain curve of the adhesive used in this analysis is shown in figure 4 (ref. 3), and is typical of the AF-127 adhesive. An adhesive thickness h_3 of 0.10 mm is used.

The variation of the shear stresses, τ_x and τ_y, with the distance from the edge of the stringer, at $y/h_2 = 0.125$ for $a/b = 0.95$, is shown in figure 5. The stresses found assuming a linear adhesive are also indicated. An applied stress level of 575 MPa is used here; this is close to the maximum stress that can be used with the AF-127 adhesive in this configuration without exceeding the adhesive failure strain. As expected, in the region near the edge of the stringer, the τ_x shear stresses found with the nonlinear adhesive behavior are considerably lower than those obtained using the linear adhesive behavior. However, the τ_y stresses are slightly higher for the nonlinear adhesive behavior. Because of the assumption in the yield criterion that the two stress components act inpendently of each other, the τ_y stresses are still behaving in a linear fashion even though in this region the adhesive layer is yielded in the x-direction. The stress level is not high enough to cause yielding in the y-direction in this instance.

Figure 6 shows the variation of the adhesive stresses near the stringer edge, at $(x-b)/h_2 = 0.37$, for the same configuration and loading used in figure 5. Again, the high τ_x stresses near the crack plane are reduced for the nonlinear adhesive. The τ_y stresses near the crack plane are also reduced compared to the linear adhesive solution.

Similar behavior of the adhesive stresses was seen for other ratios of a/b. Figures 7 and 8 show the adhesive stresses for $a/b = 1.05$, at an applied stress of 375 MPa. Figures 9 and 10 show the adhesive stresses for $a/b = 2.0$, at an applied stress of 100 MPa. Again, these applied stress levels are near to the maximum values that can be used at the given a/b value without allowing the adhesive to fail.

The larger the a/b ratio (i. e. the longer the crack), the smaller the applied stress level necessary to fail the adhesive. Thus, for applied stress levels greater than these, adhesive failure must be accounted for in the analysis. These maximum stress levels are, of course, a function of the adhesive thickness and stress-strain curve.

Figures 5, 7 and 9 show the variation in the adhesive stresses along a line parallel to the crack, at $y/h_2 = 0.125$, for a/b = 0.95, 1.05 and 2.0, respectively. Comparing these figures, we see that as the a/b ratio increases, the τ_y stresses increase in relation to the τ_x stress. When a/b is less than 1, the τ_x stress is dominant, whereas for a/b greater than 1, the τ_y is the larger of the two components. In all the cases, the nonlinear adhesive reduces the peak stresses near the stringer edge, while the stresses increase slightly in the region away from the edge of the stringer.

Figures 6, 8 and 10 show the variation in the adhesive stresses along a line parallel to the edge of the stringer, at $(x-b)/h_2 = 0.37$, for a/b = 0.95, 1.05 and 2.0, respectively. Comparing these figures, we see that the absolute magnitude of the τ_y stresses increases substantially as a/b increases. The stress in the adhesive layer increases as the crack grows towards and beneath the stringer. The value of τ_y at the stringer edge approaches 0.0 when a/b is less than 1, i.e., when the crack is not beneath the stringer. Again, the nonlinearity of the adhesive layer decreases the τ_y stresses in all cases compared to the linear adhesive values. The τ_x stresses are also decreased in the region near the centerline of the stringer but are increased slightly or remain the same away from the centerline.

The stress-intensity factors for both the linear and nonlinear adhesives are shown in figure 11. The equations for the stress-intensity factors are given in appendix A. The normalized stress-intensity factors for both the left $k_1(-a)$ and right $k_1(+a)$ crack tip are plotted versus the ratio of a/b, the half-crack length to the edge distance, for an applied stress of 100 MPa. For a/b ratios less than or equal to 1.0, when the crack has not extended beneath the stringer, the stringer does not have much effect on k_1. However, as the crack propagates beneath the stringer, the right crack-tip stress-intensity factor is reduced considerably compared to the solution for the unstiffened sheet. The presence of the stringer, though, does not have a significant effect on the left crack-tip stress-intensity factor for any ratio of a/b.

Including the nonlinearity of the adhesive has little effect on the value of k_1 for values of a/b less than 1.0. However, once the right crack tip is beneath the stringer, the effect of the stringer is reduced by the nonlinear adhesive behavior. Less load is transferred to the stringer by the nonlinear adhesive thus resulting in less decrease in the crack-tip stress-intensity factors for the nonlinear adhesive model. This appears to contradict the results reported in reference 3. However, in that reference, the solution always included debonding in both the linear and nonlinear representations of the adhesive, thus, a direct comparison cannot be made with the results of this study. The effect of the nonlinear adhesive on the stress-intensity factor at the left crack tip was much less than at the right crack tip. This is expected since $k_1(-a)$ is not as sensitive as $k_1(+a)$ to variations in the problem parameters.

CONCLUDING REMARKS

This report presents an analysis of a cracked orthotropic sheet reinforced with an adhesively bonded orthotropic semi-infinite sheet. This configuration was assumed to represent a bonded stringer when the crack is located close to the edge of the stringer. The adhesive layer is assumed to behave in a nonlinear elastic manner and to remain intact.

The effect of adhesive nonlinearity on the adhesive shear stress distribution is examined. When the adhesive is modeled with a nonlinear stress-strain curve, the peak shear stresses in the adhesive are considerably reduced in comparison to the solution for the linear elastic adhesive. Assuming a nonlinear adhesive reduces the effectiveness of the stringer in reducing the stress-intensity factors. When the adhesive behaves nonlinearly, less load is transferred from the infinite sheet to the stringer, and thus the stringer is less effective in reducing the crack-tip stress-intensity factors. The adhesive nonlinearity has less effect on the left crack-tip stress-intensity factors than on the right crack-tip stress-intensity factors, and the nonlinear adhesive does not have a significant effect on the stress-intensity factors unless the crack tip is beneath the stringer. The results of the present investigation indicate the point at which the failure of the adhesive layer must be accounted for in the analysis. The onset of adhesive failure is predicted to occur at lower applied stress levels as the crack propagates beneath the stringer.

REFERENCES

1. Arin, K.: A Plate With a Crack, Stiffened by a Partially Debonded Stringer. J. Engng. Frac. Mech. 6, pp. 133-140, 1974.

2. Swift, T.: The Effects of Fastener Flexibility And Stiffener Geometry on the Stress Intensity in Stiffened Cracked Sheet. Prospects in Fracture Mechanics, Noordhoff International Publishing Co., pp. 419-436, 1974.

3. Anderson, J. M.; Chu, C. S. and McGee, W. M.: Growth Characteristics of a Fatigue Crack Approaching and Growing Beneath an Adhesively Bonded Doubler. J. Engng. Maths. Tech. 100, pp. 52-56, 1978.

4. Hart-Smith, L. J.: Adhesive Bond Stresses and Strains at Discontinuities and Cracks in Bonded Structures. J. Engng. Tech. 100, pp. 16-24, 1978.

5. Swift, T.: Fracture Analysis of Adhesively Bonded Cracked Panels. J. Engng. Tech. 100, pp. 10-15, 1978.

6. Bigelow, C. A.: A Cracked Orthotropic Sheet Stiffened By a Semi-Infinite Orthotropic Sheet, NASA TP 2455, June 1985.

7. Poe, Jr., C. C.: A Single Fracture Toughness Parameter For Fibrous Composites. NASA TM 81911, March 1981.

8. Bigelow, C. A.: The Effect of Debond Growth on Crack Propagation in Composites Plates Reinforced With Adhesivley Bonded Composite Stringers. Ph.D. Thesis, Georgia Institute of Technology, Dec. 1984.

9. Kan, H. P.; and Ratawani, M. M.: Nonlinear Adhesive Behavior Effects in Cracked Metal-to-Composite Bonded Structures. J. Engng. Frac. Mech. 15 (1-2), pp. 123-130, 1980.

APPENDIX A
FORMUALTION OF THE GOVERNING EQUATIONS FOR THE BONDED STRINGER

This appendix presents a brief summary of the formulation of the governing equations for the linear elastic solution to the problem of the semi-infinite orthotropic sheet bonded to a cracked orthotropic sheet. The complete details can be found in reference 6.

The Integral Equations

Consider the stringer configuration shown in figure 1. The semi-infinite sheet will be referred to as a stringer for convenience. The stringer and the sheet are bonded together by an adhesive layer of constant thickness with an intact bond. The crack surfaces are subjected to a uniform pressure σ_0 and the stress state at infinity is zero as shown in figure A.1.

The integral equations are formulated under the following assumptions:

1. The sheet (layer 1), the stringer (layer 2) and the adhesive (layer 3) are homogenous and linearly elastic.

2. The sheet and the stringer are dissimilar, orthotropic materials with principal directions of orthotropy being oriented parallel and perpendicular to the crack in layer 1.

3. The thickness of the sheet h_1 and the thickness of the stringer h_2 are small compared to the in-plane dimensions so that both layers are considered to be in a state of plane stress.

4. The surface shear transmitted through the adhesive is assumed to act as a body force on the the infinite sheet and the stringer.

5. The thickness of the adhesive h_3 is small compared to the thicknesses of the sheet and stringer; thus, the adhesive layer is treated as a shear spring rather than as an elastic continuum.

The last assumption leads to the following continuity of displacement equations:

$$u_1 - u_2 = \frac{h_3}{G_3} \tau_x \qquad v_1 - v_2 = \frac{h_3}{G_3} \tau_y \tag{A.1}$$

where u_1, v_1 and u_2, v_2 are the x- and y-components of the in-plane displacement vectors in layers 1 and 2, respectively, τ_x and τ_y are the components of the adhesive shear stress, and h_3 and G_3 are the adhesive thickness and shear modulus, respectively.

From assumption 3, the two sets of body forces (force per unit volume) that act on layers 1 and 2 (see figure A.1) can be written as follows:

$$X_1 = -\frac{\tau_x}{h_1} \qquad Y_1 = -\frac{\tau_y}{h_1} \qquad X_2 = \frac{\tau_x}{h_2} \qquad Y_2 = \frac{\tau_y}{h_2} \tag{A.2}$$

Figure A.1 shows how the problem is broken into its component parts. The displacements in the sheet, shown in figure A.1, part B, and in the stringer, shown in figure A.1, part C, are determined individually. The complete expressions for these displacements are given in reference 6. Equations (A.2) are used to relate the forces X_1, Y_1, X_2, Y_2 to the adhesive shear stresses, τ_x, τ_y. The displacements for each layer are then substituted into equations (A.1) and after some algebraic manipulation, the integral equations shown below in equations (A.3) are obtained.

Thus, for the linear elastic system, the problem in figure 1 reduces to the solution of the following integral equations:

$$\frac{h_3}{G_3}\ \tau_x(x,y) + \iint_D [S_{11}(x,y,x_0,y_0)\ \tau_x(x_0,y_0) + S_{12}(x,y,x_0,y_0)\ \tau_y(x_0,y_0)]\ dx_0\ dy_0 = \sigma_0\ f_{01}(x,y) \tag{A.3}$$

$$\frac{h_3}{G_3}\ \tau_y(x,y) + \iint_D [S_{21}(x,y,x_0,y_0)\ \tau_x(x_0,y_0) + S_{22}(x,y,x_0,y_0)\ \tau_y(x_0,y_0)]\ dx_0\ dy_0 = \sigma_0\ f_{02}(x,y)$$

where D is the bonded region, and the kernels S_{jk} (j,k=1,2) and the functions f_{01} and f_{02} are known (see ref. 6 for details). The kernels S_{jk} are related to the distributed body force loadings shown in figure A.1, parts B and C, and are functions of the material properties of each layer, the half crack length a and the stringer edge distance b. The functions f_{01} and f_{02} are related to the uniform crack face pressure σ_0 shown in figure A.1, part B, and are functions of the material properties of layer 1 and the half crack length a.

The Stress-Intensity Factor Equations

In the present problem, due to symmetries in the geometry and the loading, the shear component of the stress-intensity factor is zero. The normal component is found by combining the effects of the crack-face pressure σ_0 and the adhesive shear forces τ_x and τ_y acting on the sheet. The stress-intensity factor may be expressed in terms of the unknowns τ_x and τ_y as follows:

$$k_1(a_0) = \sigma_0\sqrt{a} + \frac{2a_0}{a_0\sqrt{a}\,h_1} \iint_D [W_1(x,y,x_0,y_0)\ \tau_x(x_0,y_0) + W_2(x,y,x_0,y_0)\ \tau_y(x_0,y_0)]\ dx_0\ dy_0 \qquad (A.4)$$

where

a_0 = +a for the right crack tip

= -a for the left crack tip

The terms W_1 and W_2 are functions of the crack length, edge distance of the stringer and the material properties of layer 1. Complete details on the derivation of the equation for the stress-intensity factors are given in reference 6.

The solution of equations (A.3) gives the stress distribution in the adhesive, $\tau_x(x,y)$ and $\tau_y(x,y)$. Using these adhesive shear stresses in equation (A.4), the stress-intensity factors at either crack tip can be determined.

Table I - Material Properties (ref. 7)

Layer No.	E_x (GPa)	E_y (GPa)	ν_{xy}	G_{xy} (GPa)
1	51.40	51.40	0.30650	19.67
2	10.86	129.40	0.02617	5.70

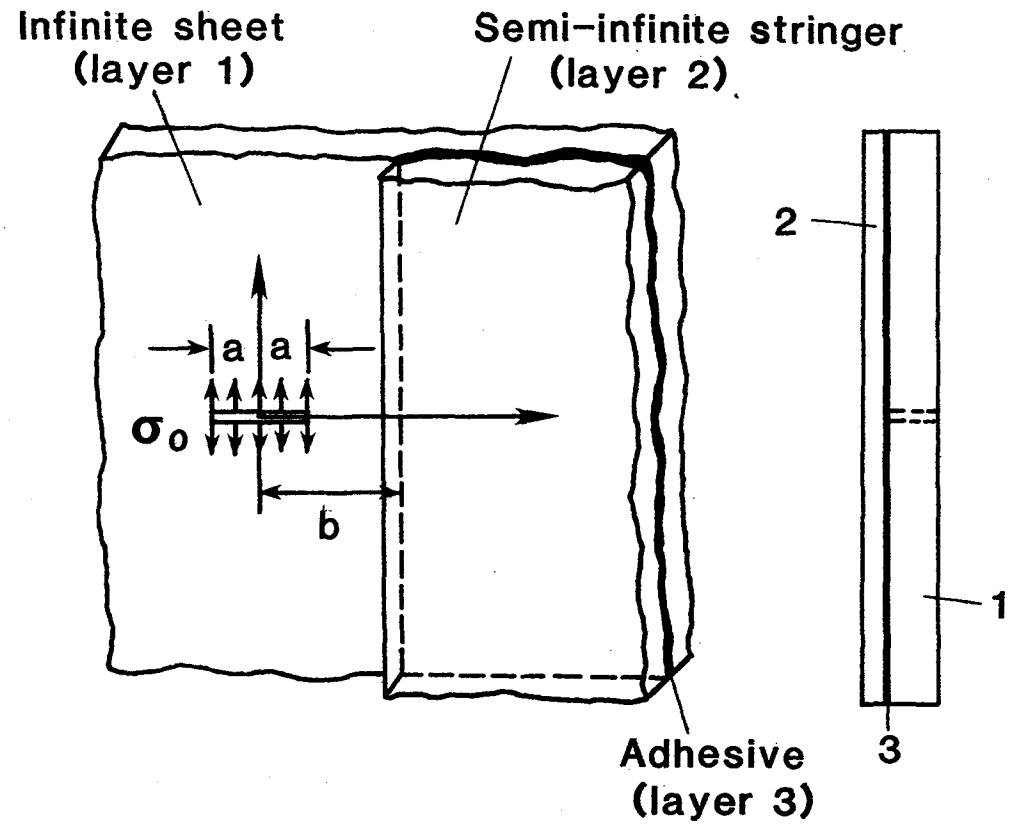

Figure 1. Problem configuration.

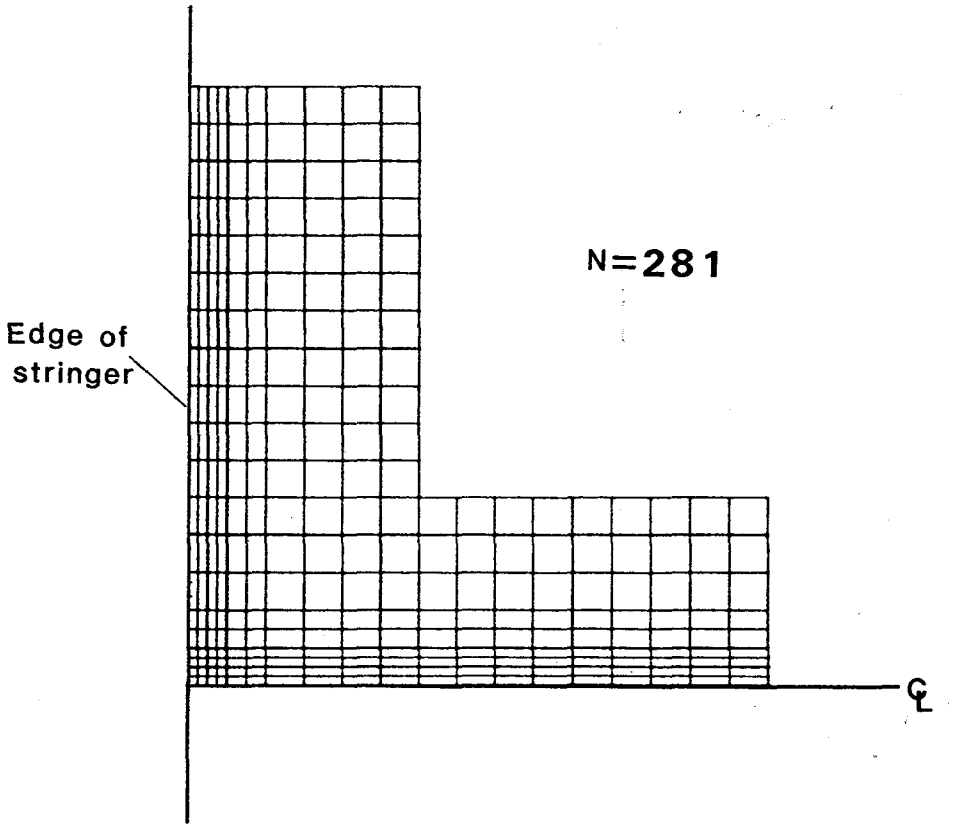

Figure 2. Typical mesh used in numerical integration.

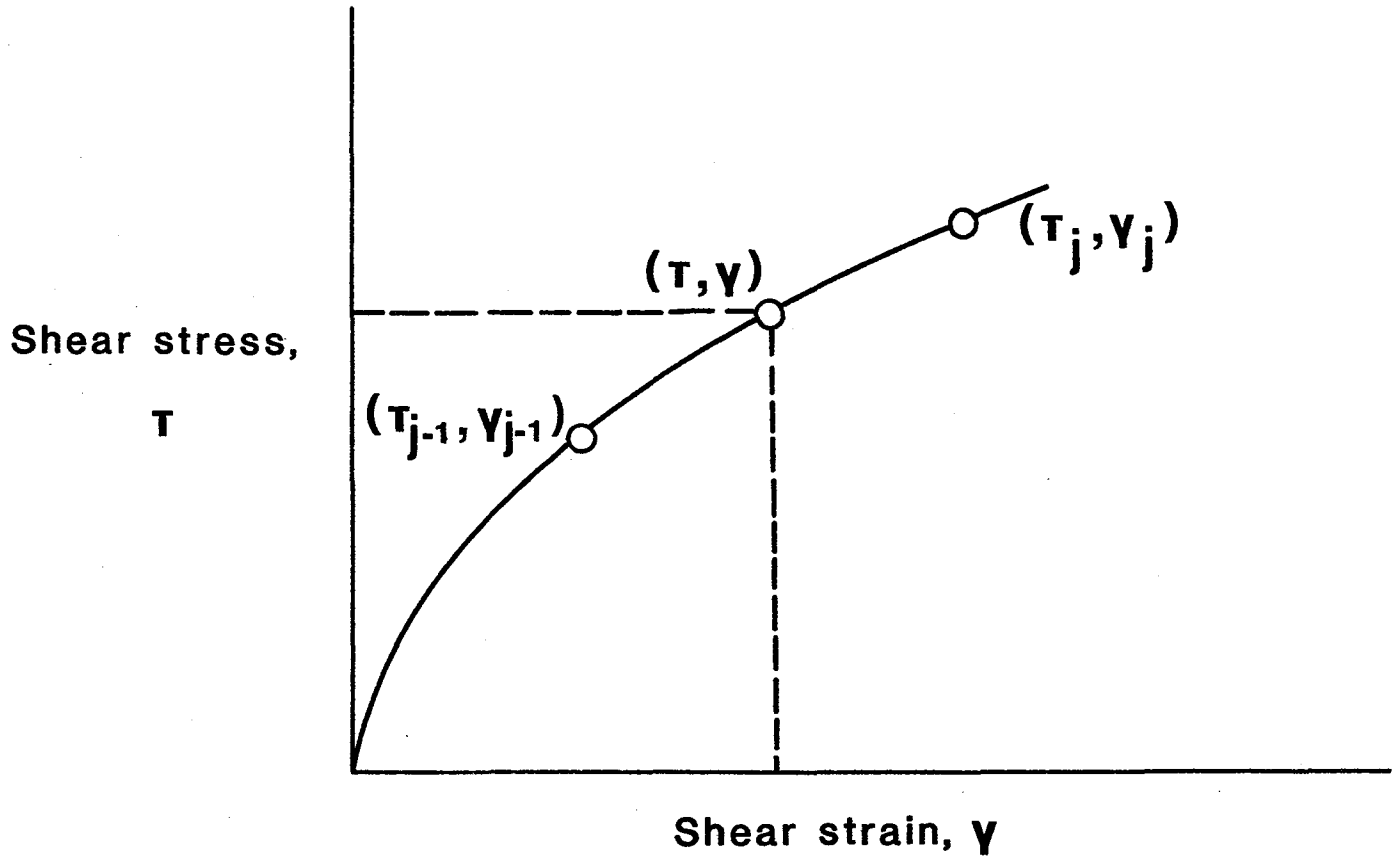

Figure 3. Schematic stress-strain curve.

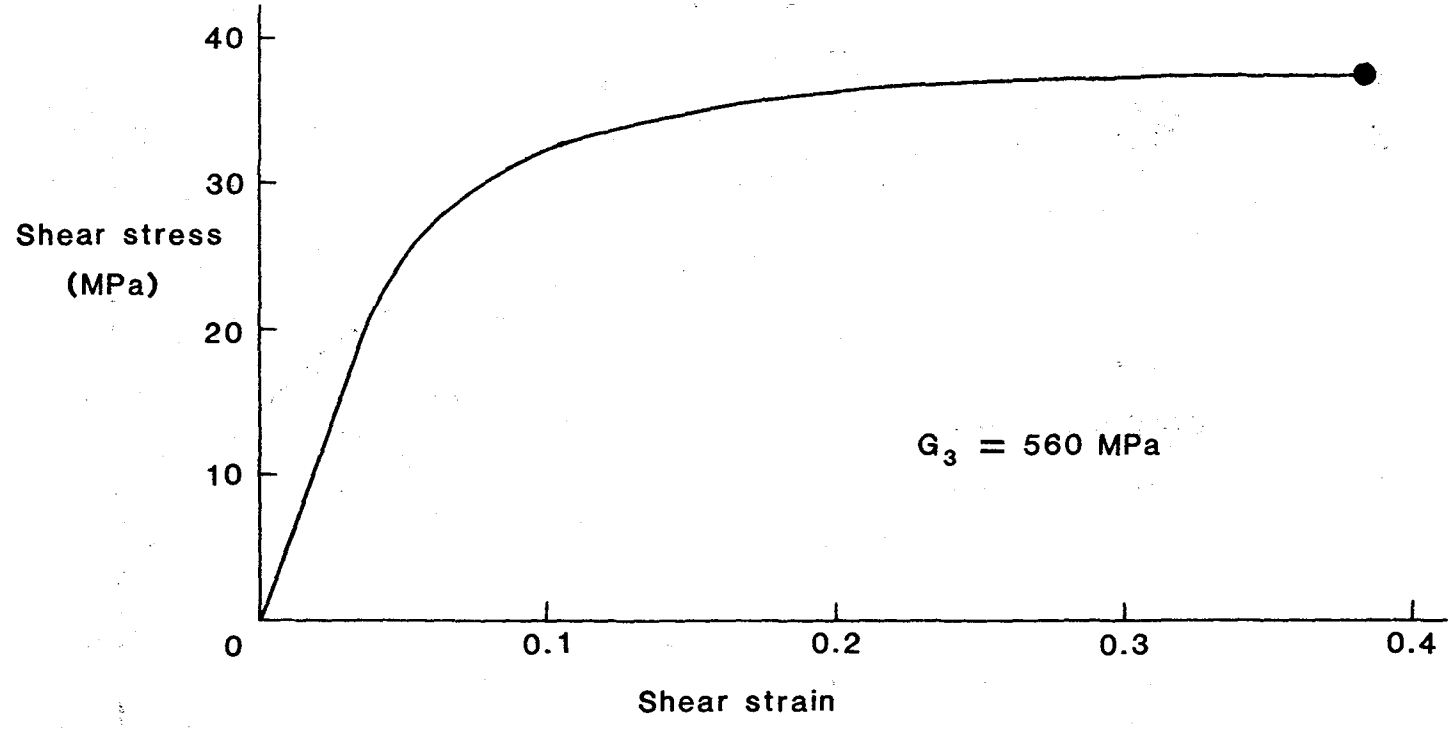

Figure 4. Adhesive shear stress-strain curve, AF-127.

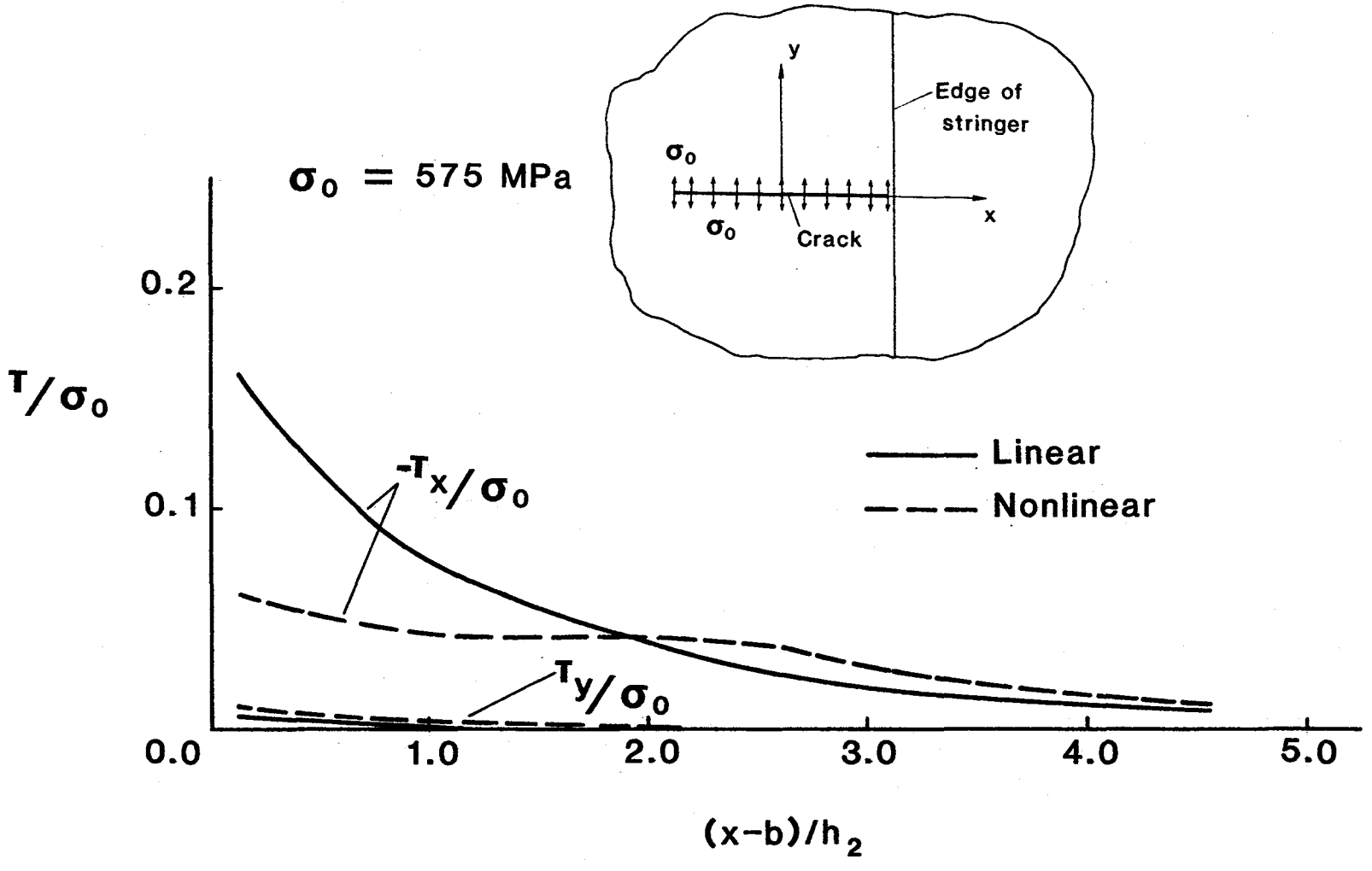

Figure 5. Adhesive stress distribution near crack plane at $y/h_2 = 0.125$ for $a/b = 0.95$.

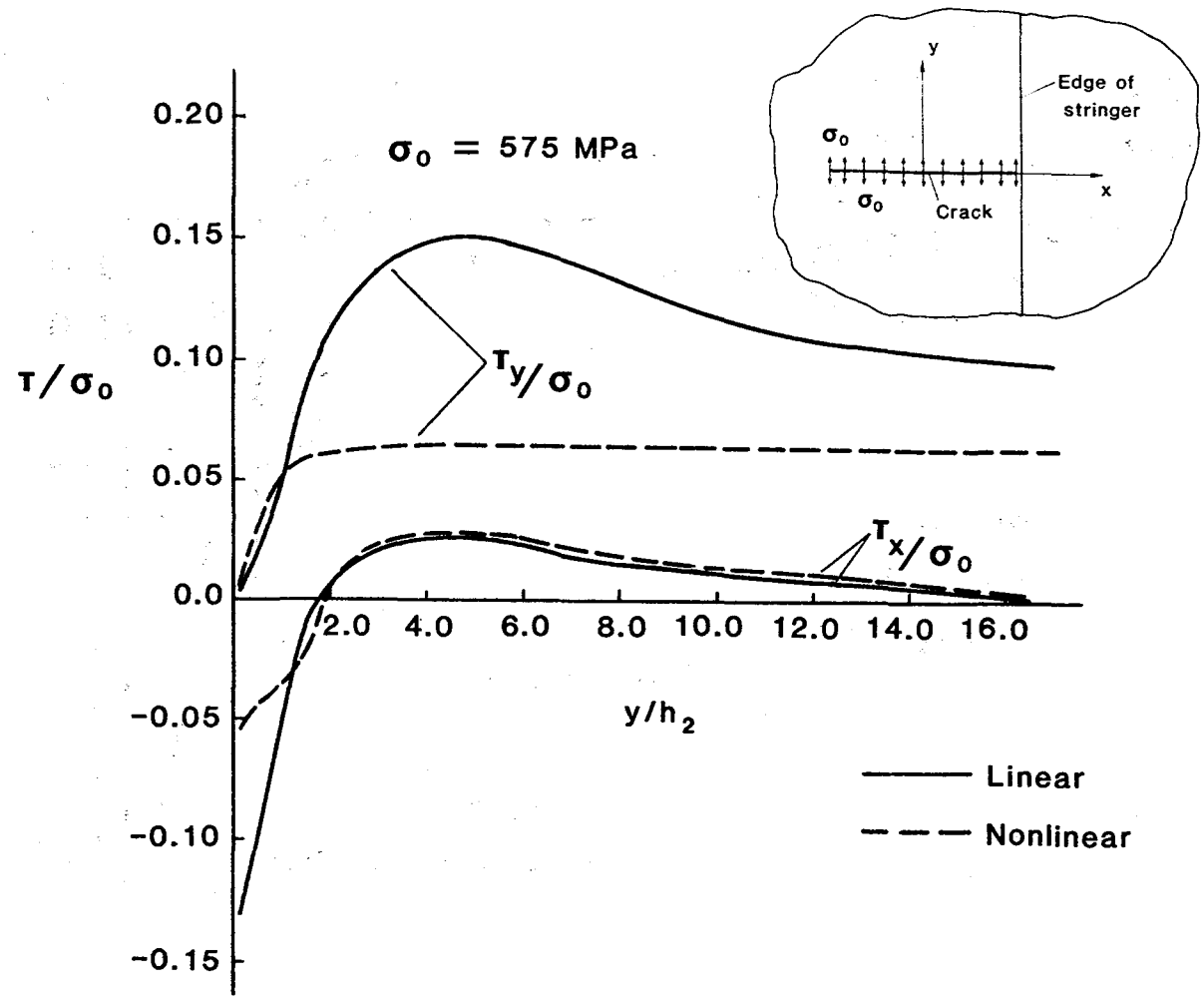

Figure 6. Adhesive stress distribution near stringer edge at $(x-b)/h_2 = 0.37$ for $a/b = 0.95$.

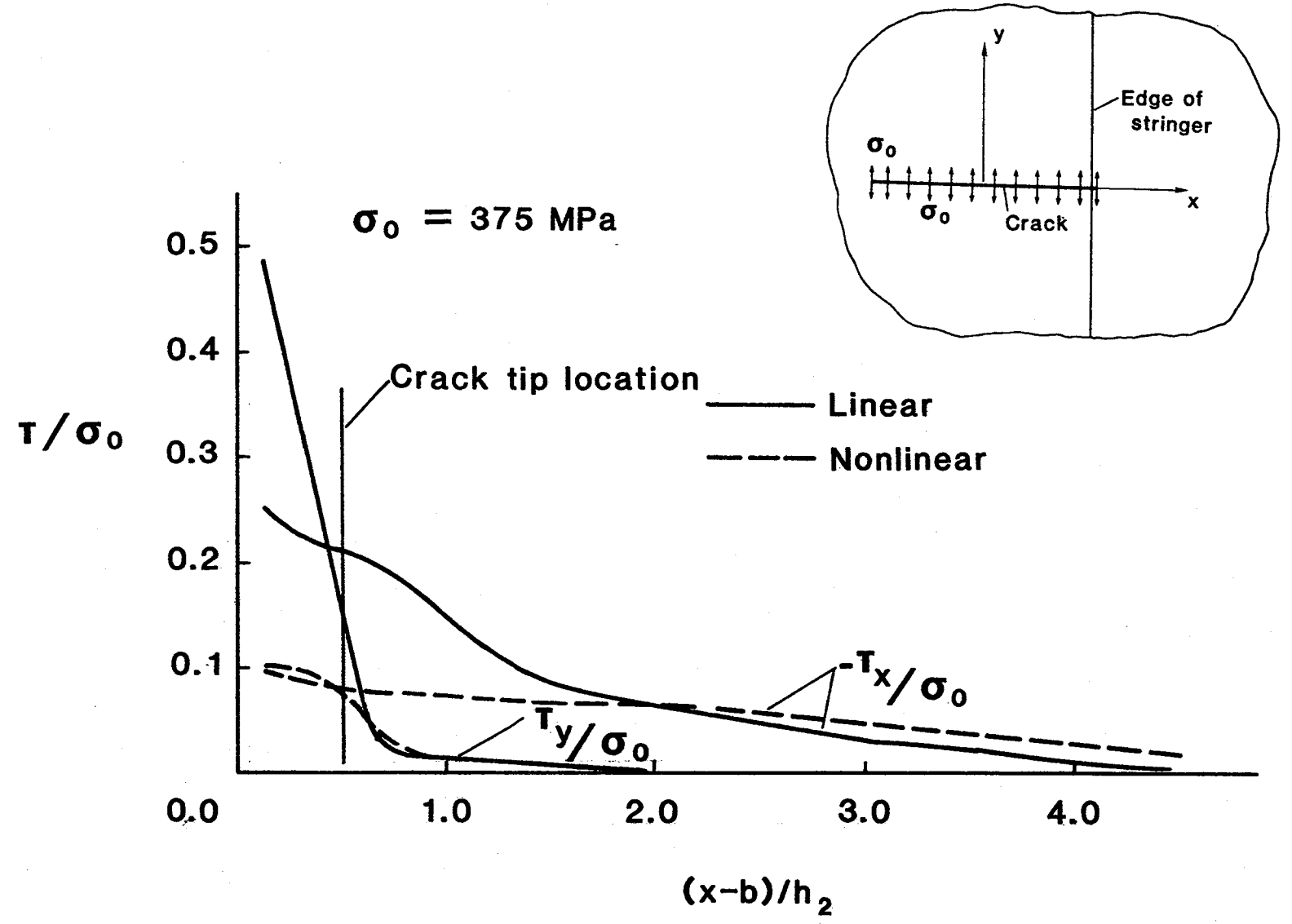

Figure 7. Adhesive stress distribution near crack plane at $y/h_2 = 0.125$ for $a/b = 1.05$.

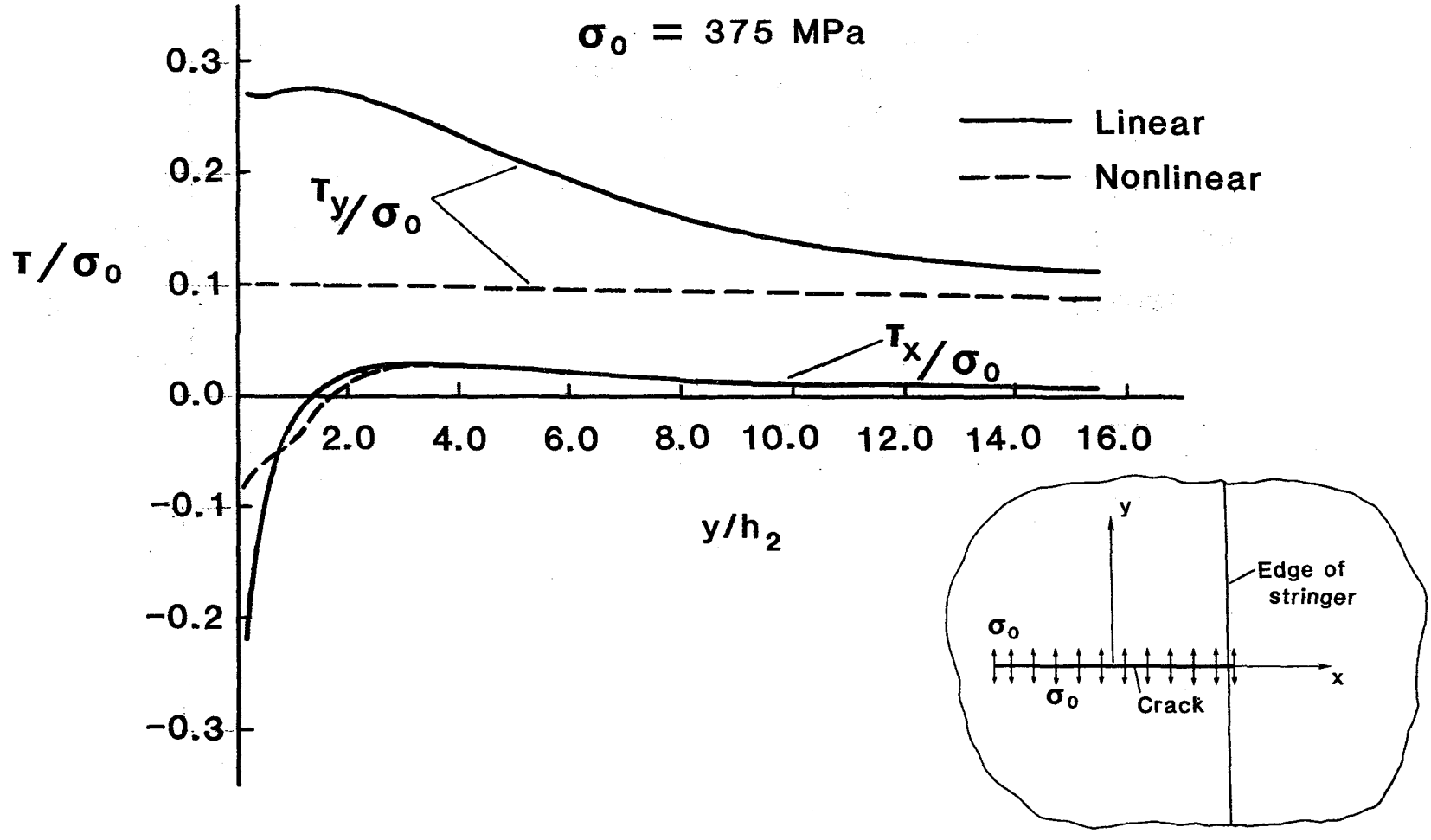

Figure 8. Adhesive stress distribution near stringer edge at $(x-b)/h_2$ = 0.37 for a/b = 1.05.

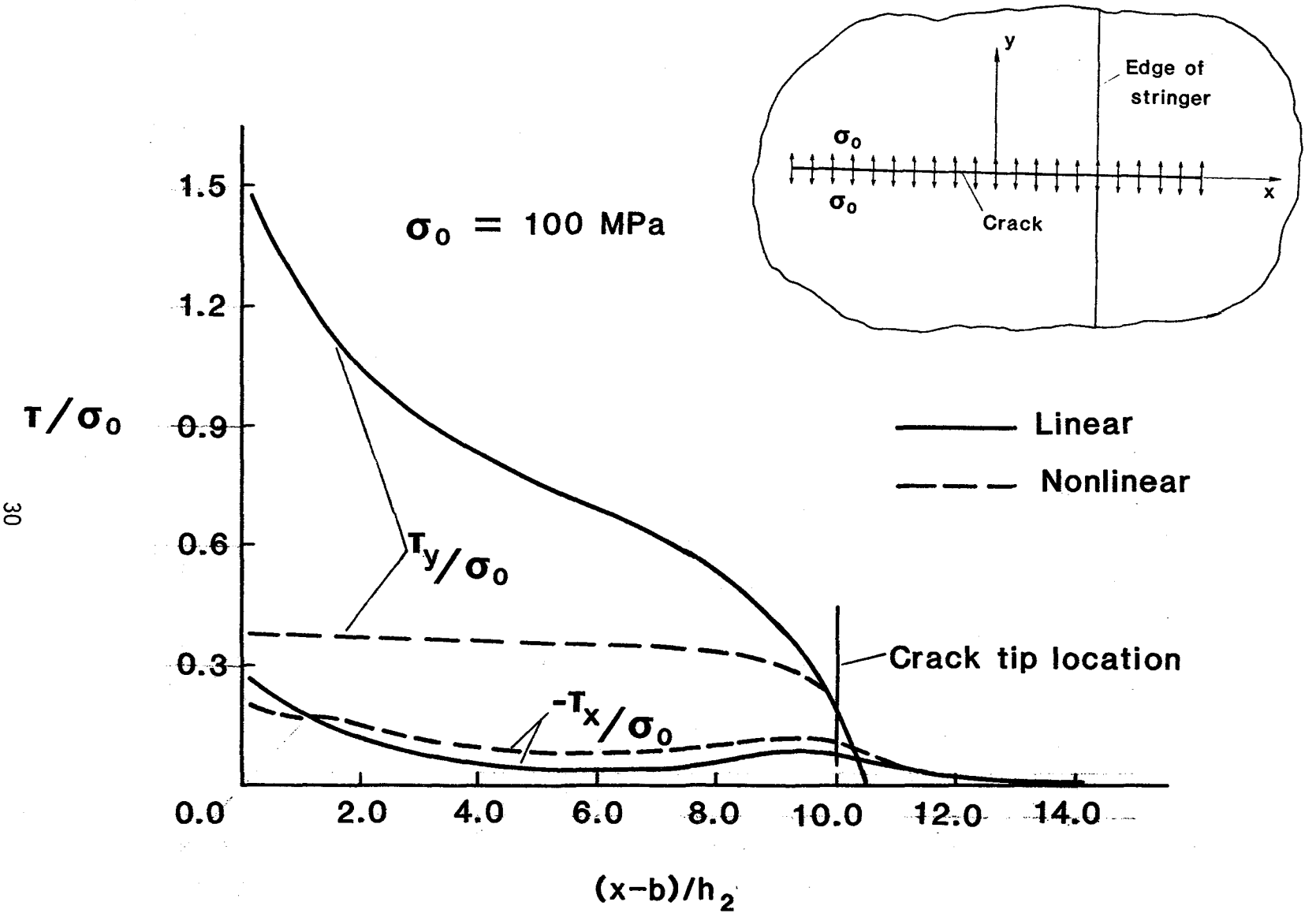

Figure 9. Adhesive stress distribution near crack plane at $y/h_2 = 0.125$ for $a/b = 2.0$.

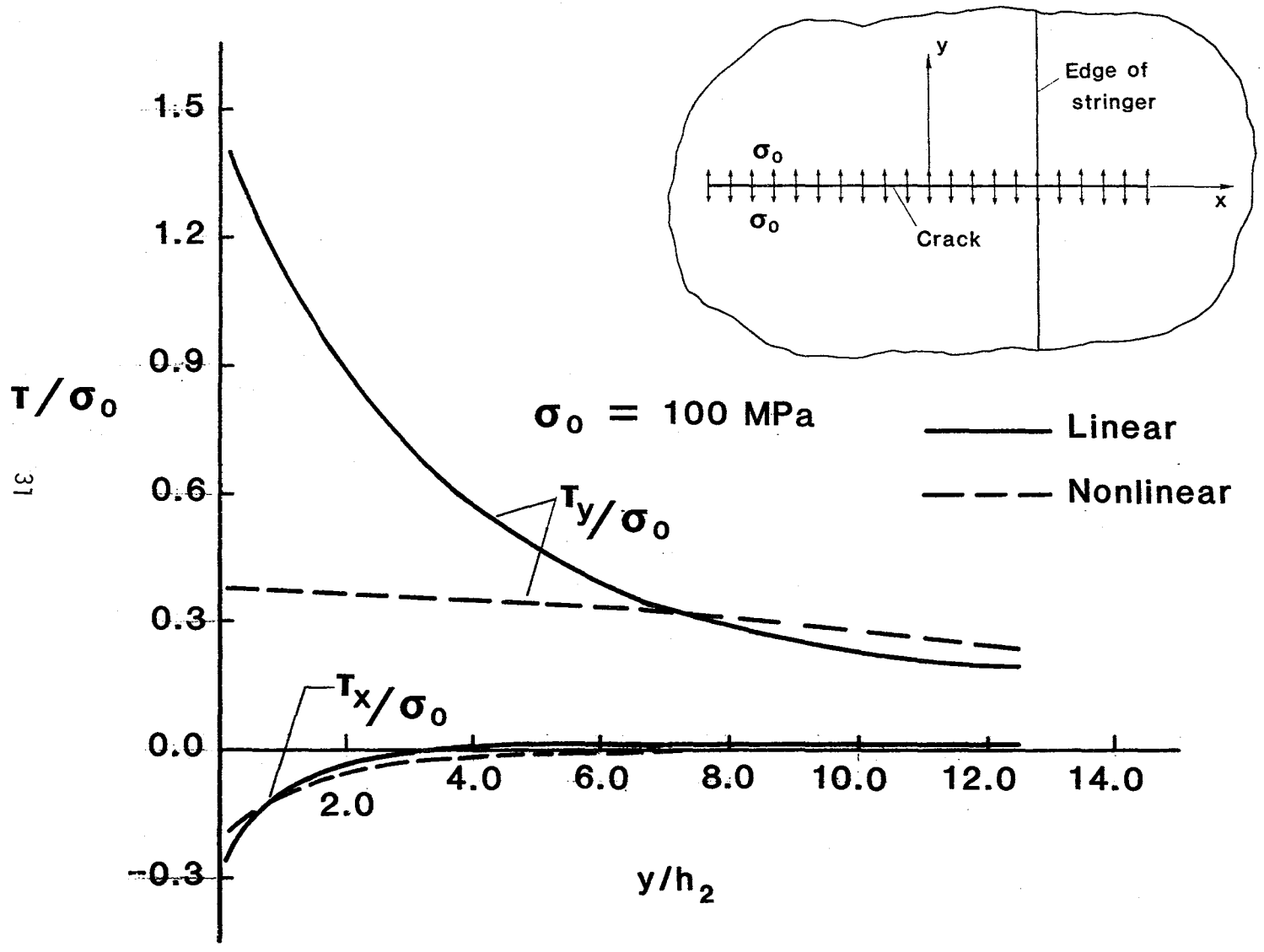

Figure 10. Adhesive stress distribution near stringer edge at $(x-b)/h_2 = 0.37$ for $a/b = 2.0$.

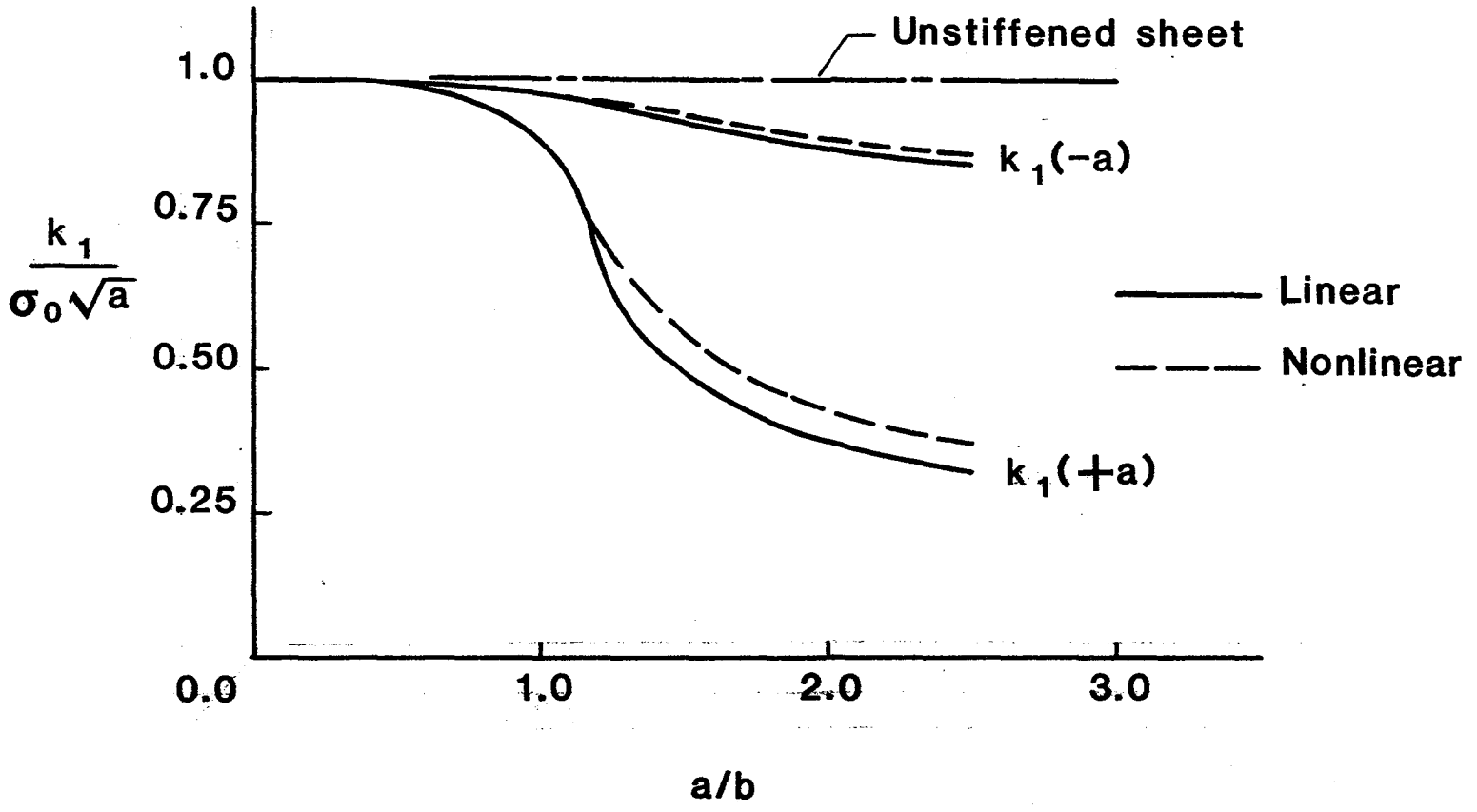

Figure 11. Effect of adhesive nonlinearity on stress-intensity factors.

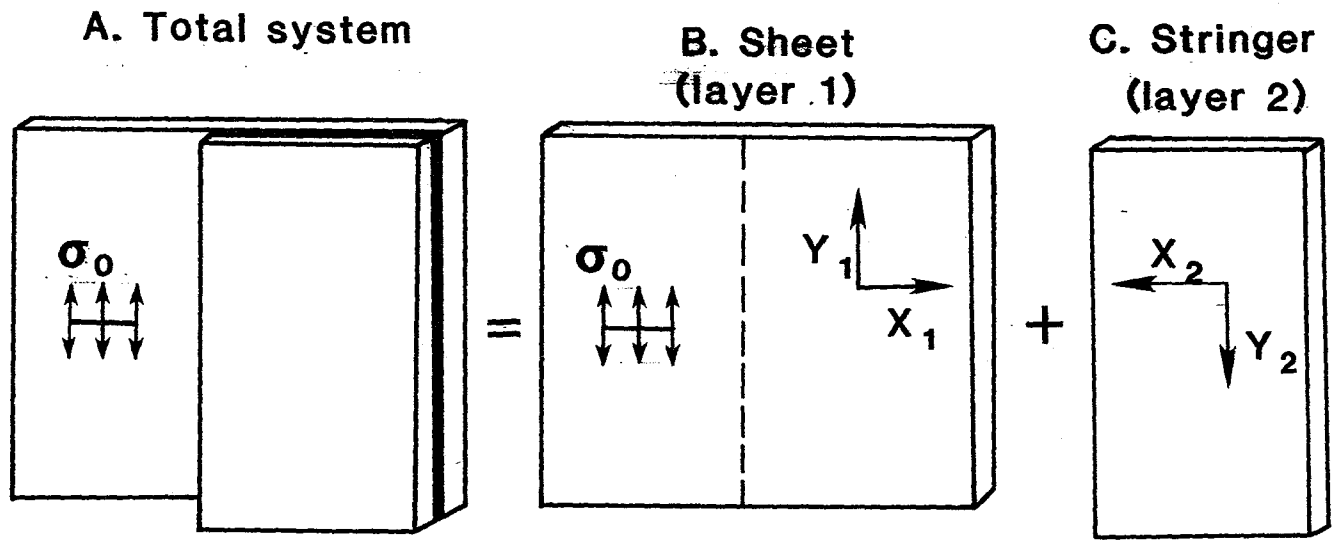

Figure A.1. Superposition model of the problem.

1. Report No.	2. Government Accession No.	3. Recipient's Catalog No.
NASA TM-87584		

4. Title and Subtitle	5. Report Date
Nonlinear Adhesive Behavior Effects in a Cracked Orthotropic Sheet Stiffened by a Semi-Infinite Orthotropic Sheet	August 1985
	6. Performing Organization Code: 506-53-23

7. Author(s)	8. Performing Organization Report No.
C. A. Bigelow	

9. Performing Organization Name and Address	10. Work Unit No.
NASA Langley Research Center Hampton, VA 23665	11. Contract or Grant No.

12. Sponsoring Agency Name and Address	13. Type of Report and Period Covered
National Aeronautics and Space Administration Washington, DC 20546	Technical Memorandum
	14. Sponsoring Agency Code

15. Supplementary Notes

16. Abstract

The stress-intensity factors are determined for a cracked orthotropic sheet adhesively bonded to an orthotropic stringer where the adhesive layer is modeled with a nonlinear stress-strain curve. Since the stringer is modeled as a semi-infinite sheet, the solution is most appropriate for a crack tip located near a stringer edge. By the use of Green's functions and the complex variable theory of orthotropic elasticity developed by Lekhnitskii, a set of integral equations is obtained. The integral equations are replaced by an equivalent set of algebraic equations, which are solved to obtain the shear stress distribution in the adhesive layer. With these adhesive stresses, the crack-tip stress-intensity factors are found.

When the adhesive was modeled with a nonlinear stress-strain curve, the peak shear stresses in the adhesive were considerably reduced in comparison to the solution for the linear elastic adhesive. This resulted in increases in the stress-intensity factors for the nonlinear adhesive solution compared to the linear adhesive solution. The nonlinear adhesive did not have a significant effect on the stress-intensity factor unless the near crack tip was beneath the stringer. The present investigation assumes that the adhesive bond remains intact. Onset of adhesive failure is predicted to occur at decreasing levels of applied stress as the crack propagates beneath the stringer.

17. Key Words (Suggested by Author(s))	18. Distribution Statement
Nonlinear Integral equations Stress-intensity factors Adhesive stresses Composites Orthotropic	Unclassified - Unlimited Subject Category 39

19. Security Classif. (of this report)	20. Security Classif. (of this page)	21. No. of Pages	22. Price
Unclassified	Unclassified	34	A03

For sale by the National Technical Information Service, Springfield, Virginia 22161